(Received 21 October 2023, Accepted 4 March 2024, Scheduled 28 August 2024)

Deviation Analysis of Multiport VNA Hardware Specification-Related Nonideality

Nan Sun[1,*], Liang Ren[2], Zhi-Tao Yang[2], Ming Shen[3], and Hong-Wei Deng[1]

[1] College of Electronic and Information Engineering, Nanjing University of Aeronautics and Astronautics, Nanjing, China
[2] Science and Technology on Space Physics Laboratory, Beijing, China
[3] Department of Electronic Systems, Aalborg University, Aalborg, Denmark

ABSTRACT: In this paper, the deviation generated by actual multiport vector network analyzer (MVNA) hardware specification is derived. Based on the error flowchart of the n-port VNA, the generalized matrix expression of the raw scattering parameters for each error term is solved by introducing the generalized node method. Combined with incremental method, the generalized matrix expression of the final relative scattering parameter measurement deviation is calculated after ignoring the infinitesimals above the second order. Thus, the method of variable controlling is applied to make difference so that the deviation associated with every error term can be obtained. The validness and effectiveness of this method are verified by utilizing Agilent N5230C to measure a 20 dB direction coupler. The data is processed with an algorithm in MATLAB.

1. INTRODUCTION

Due to the wide application of RF and microwave devices in the fields of wireless communication, vector network analyzer (VNA) has become one of the most essential measuring instruments in microwave engineering. To realize such a goal, software and hardware-related improvement should both be made.

Enhancing the accuracy of measurement in the aspect of software is an excellent choice of cost performance [1–8]. The first commercial calibration standard was proposed in 1968, which is based on a 12-term model of error propagation. This short-open-load-through (SOLT) calibration method has become popular even to this day [1], with all included terms mapped to 12 hardware specifications. However, the general situation where the calibration sets are non-ideal is supposed to be taken into account because their reflection coefficients would usually deviate inevitably from the ideal specifications [9–13]. Intuitively, to optimize the effectiveness and efficiency of calibration, the contributions of the nonideality of reflection coefficients were derived by Stumper in SOLT calibration process applying the partial derivative method in [2, 3]. But there is not much literature on multiport VNA (MVNA) published until the late 1990s [11–17] because of its complex structure.

Similar to two-port VNA, effort in terms of hardware should also be made, whose expense is much higher than that related to software though. In attempt to find a considerably cost-effective solution to improve the MVNA performance at the hardware level, the deviation related to MVNA hardware specification contributor can be derived, served as a guidance to efficiently clarify the prior hardware MVNA parts, so that those less demanding could then be processed with less rigorous standards.

In this paper, deviation analysis of MVNA hardware specification-related nonideality is conducted. Based on the error model of the n-port MVNA, the generalized matrix expression of the raw S-parameters for each error term is calculated by introducing the generalized node method. Combined with incremental method, the generalized matrix expression of the final relative scattering parameter measurement deviation is calculated after ignoring the infinitesimals above the second order. Statistical analysis is done, and a demand priority of MVNA specifications is presented as a cheap yet efficient guidance to design MVNA.

2. CONTRIBUTORS OF DEVIATION

2.1. The Corresponding Relation between MVNA Hardware Specification and Terms of Error

As shown in Fig. 1, a $3n^2$-term error flowgraph is considered in GSOLT calibration for MVNA, including the forward and reverse directivity errors ($E_{Di/j}$) generated by the directivity nonideality of the coupler/power divider inside MVNA, forward and reverse reflection tracking errors ($E_{Ri/j}$) caused by electric length difference of the receiver channels of Port i and Port j, forward and reverse source match errors ($E_{Si/j}$), forward and reverse transmission tracking errors ($E_{Tji/ij}$) caused by untracked changes of frequency-dependent amplitude/phase and the electric length of two channels, forward and reverse load match errors ($E_{Lji/ij}$) caused by mismatch of the unexcited port and, at last, forward and reverse crosstalk errors ($E_{Xji/ij}$) at Ports 1 and 2, respectively. By applying GSOLT

* Corresponding author: Nan Sun (897943212@qq.com).

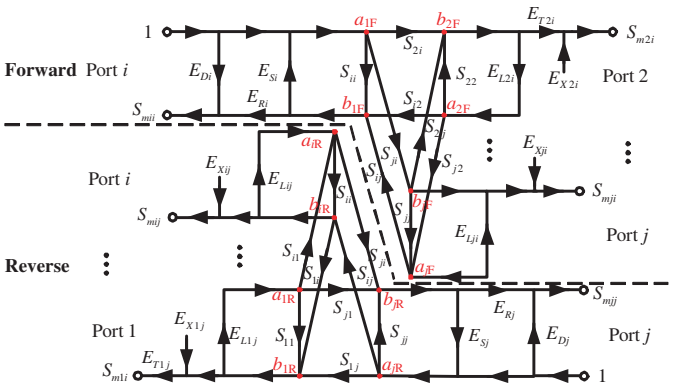

FIGURE 1. $3n^2$ error term model of MVNA ($i, j \in [1, n], i \neq j$).

calibration steps, all mentioned error terms can be measured and so does S-parameters $S_{mii/ji}$.

According to the definition of scattering matrix, an equation set can be obtained as

$$\begin{cases} [b_i] = [S]\,[a_i] \\ [a_i] = [I_i] + [E_{SLi}]\,[E_{RTi}]^{-1}\,([S_{mi}] - [E_{DXi}]) \\ [b_i] = [E_{RTi}]^{-1}\,([S_{mi}] - [E_{DXi}]) \end{cases} \tag{1}$$

while

$$[a_i] = \begin{bmatrix} a^i_{1\mathrm{F/R}} \\ a^i_{2\mathrm{F/R}} \\ \vdots \\ a^i_{n\mathrm{F/R}} \end{bmatrix}, \quad [b_i] = \begin{bmatrix} b^i_{1\mathrm{F/R}} \\ b^i_{2\mathrm{F/R}} \\ \vdots \\ b^i_{n\mathrm{F/R}} \end{bmatrix}, \quad [I_i] = \begin{bmatrix} 0 \\ \vdots \\ 1(\text{row } i) \\ \vdots \\ 0 \end{bmatrix},$$

$$[E_{DXi}] = \begin{bmatrix} E_{X1i} \\ \vdots \\ E_{Di} \\ \vdots \\ E_{Xni} \end{bmatrix}, \quad [S_{mi}] = \begin{bmatrix} S_{m1i} \\ \vdots \\ S_{mni} \end{bmatrix}$$

$$[E_{SLi}] = \begin{bmatrix} E_{L1i} & & & \\ & \ddots & & \\ & & E_{Si} & \\ & & & \ddots \\ & & & E_{Lni} \end{bmatrix},$$

$$[E_{RTi}] = \begin{bmatrix} E_{T1i} & & & \\ & \ddots & & \\ & & E_{Ri} & \\ & & & \ddots \\ & & & E_{Tni} \end{bmatrix}$$

By applying Equation (1), scattering matrix $[S]$ can be expressed as

$$\begin{aligned} &[E_{RTi}]^{-1}\left\{\overrightarrow{S_{mi}} - [E_{DXi}]\right\} \\ &= [S]\left\{\overrightarrow{I_i} + [E_{SLi}]\,[E_{RTi}]^{-1}\left(\overrightarrow{S_{mi}} - [E_{DXi}]\right)\right\} \end{aligned} \tag{2}$$

In the end, its analytical expression is

$$[S] = \begin{bmatrix} S_{11} & S_{12} & S_{13} & S_{14} \\ S_{21} & S_{22} & S_{23} & S_{24} \\ S_{31} & S_{32} & S_{33} & S_{34} \\ S_{41} & S_{42} & S_{43} & S_{44} \end{bmatrix}$$

$$= \begin{bmatrix} \frac{S_{m11}-E_{D1}}{E_{R1}} & \frac{S_{m12}-E_{X12}}{E_{T12}} & \frac{S_{m13}-E_{X13}}{E_{T13}} & \frac{S_{m14}-E_{X14}}{E_{T14}} \\ \frac{S_{m21}-E_{X21}}{E_{T21}} & \frac{S_{m22}-E_{D2}}{E_{R2}} & \frac{S_{m23}-E_{X23}}{E_{T23}} & \frac{S_{m24}-E_{X24}}{E_{T24}} \\ \frac{S_{m31}-E_{X31}}{E_{T31}} & \frac{S_{m32}-E_{X32}}{E_{T32}} & \frac{S_{m33}-E_{D3}}{E_{R3}} & \frac{S_{m34}-E_{X34}}{E_{T31}} \\ \frac{S_{m41}-E_{X41}}{E_{T41}} & \frac{S_{m42}-E_{X42}}{E_{T42}} & \frac{S_{m43}-E_{X43}}{E_{T43}} & \frac{S_{m44}-E_{D4}}{E_{R4}} \end{bmatrix}$$

$$\times \begin{bmatrix} S_{m11}\frac{E_{S1}}{E_{R1}}+1 & S_{m12}\frac{E_{L12}}{E_{T12}} & S_{m13}\frac{E_{L13}}{E_{T13}} & S_{m14}\frac{E_{L14}}{E_{T14}} \\ S_{m21}\frac{E_{L21}}{E_{T21}} & S_{m22}\frac{E_{S2}}{E_{R2}}+1 & S_{m23}\frac{E_{L23}}{E_{T23}} & S_{m24}\frac{E_{L24}}{E_{T24}} \\ S_{m31}\frac{E_{L31}}{E_{T31}} & S_{m32}\frac{E_{L32}}{E_{T32}} & S_{m33}\frac{E_{S3}}{E_{R3}}+1 & S_{m34}\frac{E_{L34}}{E_{T34}} \\ S_{m41}\frac{E_{L41}}{E_{T41}} & S_{m42}\frac{E_{L42}}{E_{T42}} & S_{m43}\frac{E_{L43}}{E_{T43}} & S_{m44}\frac{E_{S4}}{E_{R4}}+1 \end{bmatrix}^{-1} \tag{3}$$

2.2. Influence on Raw Measured *S*-Parameters

It is easy to tell that the traditional derivate method for two-port VNA deviation analysis would be infeasible in the case of MVNA deviation analysis. High order inverse operation of matrix is required. An alternative method is herein introduced to efficiently calculate the hardware-related deviations of MVNA.

In actual measurement of the device/network under test (DUT) utilizing MVNA, the raw measurement S-parameters $S_{mii/ji/jj/ij}$ can be measured first before calibration, which makes them considered as known values. By applying GSOLT measurement steps (not calibration steps), all the error terms x_k can be calculated and, naturally, should be treated as known values. After serving GSOLT calibration steps, the final/calibrated

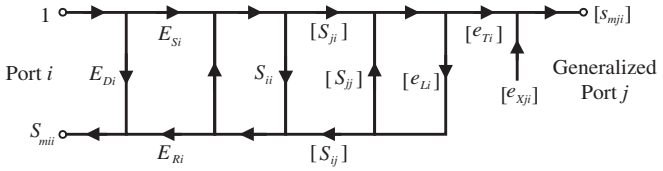

FIGURE 2. $3n^2$ error term generalized nodal model of MVNA (Port i excited).

S-parameters $S_{cii/ji/jj/ij}$ can also be measured. After the preliminary preparation, a flowgraph of alternative operation model is established, as shown in Fig. 2. According to generalized nodal theory, the raw generalized scattering matrix can be expressed as

$$\begin{cases} S_{mii} = M_{ii} = E_{Di} + E_{Ri}H_i\left(1 - E_{Si}H_i\right)^{-1} \\ [s_{mji}] = [e_{Xi}] + [M_{ji}] = [e_{Xi}] + [e_{Ti}]\,[G_i]\left(1 - E_{Si}H_i\right)^{-1} \\ i, j = 1 \sim n \text{ and } i \neq j \\ \text{and in which} \\ M_{ii} = E_{Di} + E_{Ri}H_i\left(1 - E_{Si}H_i\right)^{-1}, \\ [M_{ji}] = [e_{Ti}]\,[G_i]\left(1 - E_{Si}H_i\right)^{-1} \\ [G_i] = \left([I]_{(n-1)\times(n-1)} - [e_{Li}]\,[s_{jj}]\right)^{-1}[s_{ji}], \\ H_i = S_{ii} + [s_{ij}]\,[e_{Li}]\,[G_i] \end{cases} \tag{4}$$

and generalized raw transmission matrix $[s_{mji}]$, generalized final transmission matrix $[s_{ji/ij}]$, generalized crosstalk error matrix $[e_{Xi}]$, generalized crosstalk error matrix $[e_{Li}]$, and generalized crosstalk error matrix $[e_{Ti}]$ are

$$[s_{mji}] = \begin{bmatrix} S_{m1i} \\ \vdots \\ S_{m(j-1)i} \\ S_{m(j+1)i} \\ \vdots \\ S_{mni} \end{bmatrix}, \quad [s_{ji}] = \begin{bmatrix} S_{1i} \\ \vdots \\ S_{(j-1)i} \\ S_{(j+1)i} \\ \vdots \\ S_{ni} \end{bmatrix},$$

$$[s_{ij}] = \begin{bmatrix} S_{i1} \\ \vdots \\ S_{i(j-1)} \\ S_{i(j+1)} \\ \vdots \\ S_{in} \end{bmatrix}^T, \quad [e_{Xi}] = \begin{bmatrix} E_{X1i} \\ \vdots \\ E_{X(i-1)i} \\ E_{X(i+1)i} \\ \vdots \\ E_{Xni} \end{bmatrix}$$

$$[s_{jj}] = \begin{bmatrix} S_{11} & \cdots & S_{1(i-1)} & S_{1(i+1)} & \cdots & S_{1n} \\ \vdots & \ddots & \vdots & \vdots & \iddots & \vdots \\ S_{(i-1)1} & \cdots & S_{(i-1)(i-1)} & S_{(i-1)(i+1)} & \cdots & S_{(i-1)n} \\ S_{(i+1)1} & \cdots & S_{(i+1)(i-1)} & S_{(i+1)(i+1)} & \cdots & S_{(i+1)n} \\ \vdots & \iddots & \vdots & \vdots & \ddots & \vdots \\ S_{n1} & \cdots & S_{n(i-1)} & S_{n(i-1)} & \cdots & S_{nn} \end{bmatrix},$$

$$[e_{Li}] = \begin{bmatrix} E_{L1i} & & & & & \\ & \ddots & & & & \\ & & E_{L(i-1)i} & & & \\ & & & E_{L(i+1)i} & & \\ & & & & \ddots & \\ & & & & & E_{Lni} \end{bmatrix},$$

$$[e_{Ti}] = \begin{bmatrix} E_{T1i} & & & & & \\ & \ddots & & & & \\ & & E_{T(i-1)i} & & & \\ & & & E_{T(i+1)i} & & \\ & & & & \ddots & \\ & & & & & E_{Tni} \end{bmatrix} \tag{5}$$

As the nodal expression is given, the deviation caused by individual errors can be obtained by simple differential method

$$\begin{cases} \Delta S_{mii}\left(\Delta x_k\right) = S_{mii}^{x_k^{real}} - S_{mii}^{x_k^{ideal}} \\ = \left\{E_{Di} + E_{Ri}H\left(1 - E_{Si}H\right)^{-1}\right\}_{x_k = x_k^{real}} \\ - \left\{E_{Di} + E_{Ri}H\left(1 - E_{Si}H\right)^{-1}\right\}_{x_k = x_k^{ideal}} \\ [\Delta s_{mji}\left(\Delta x_k\right)] = \left[s_{mji}^{x_k^{real}}\right] - \left[s_{mji}^{x_k^{ideal}}\right] \\ = \left\{[e_{Xi}] + [e_{Ti}]\,[G]\left(1 - E_{Si}H\right)^{-1}\right\}_{x_k = x_k^{real}} \\ - \left\{[e_{Xi}] + [e_{Ti}]\,[G]\left(1 - E_{Si}H\right)^{-1}\right\}_{x_k = x_k^{ideal}} \end{cases} \tag{6}$$

while $S_{mii}^{x_k^{real}}/[s_{mji}^{x_k^{real}}]$ and $S_{mii}^{x_k^{ideal}}/[s_{mji}^{x_k^{ideal}}]$ represent the calculated raw measured S-parameter (by Equation (2)) based on real (x_k^{real}) and ideal (x_k^{ideal}) values of every error term x_k, respectively.

2.3. Influence on Final Measured *S*-Parameters

However, the corrected/calibrated S-parameters matter more because most deviations have been removed during calibration. So, remaining deviations of corrected S-parameters need to be reconsidered.

Considering the complex Equation (3), the incremental method and generalized nodal equation are combined to analyze MVNA hardware-related deviation, which, to some extent, is an approximation after ignoring infinitesimals above the second order. By applying incremental method to Equation (1), we have

$$\begin{cases} [b_i] + [\Delta b_i] = [S + \Delta S]\left([a_i] + [\Delta a_i]\right) \\ [a_i] + [\Delta a_i] = [I_i] + [E_{SLi} + \Delta E_{SLi}] \\ \qquad [E_{RTi} + \Delta E_{RTi}]^{-1}\left([S_{mi}] - [E_{DXi}]\right) \\ [b_i] + [\Delta b_i] = [E_{RTi} + \Delta E_{RTi}]^{-1} \\ \qquad \{S_{mi} - [E_{DXi} + \Delta E_{DXi}]\} \end{cases} \tag{7}$$

while Δ represents the increment.

A difference function set can be obtained by subtracting Equation (1) from (7), which can be ultimately expressed as

$$\begin{cases} \Delta S_{kl}\left(\Delta E_i\right) = \left.\begin{array}{l} d_{il}\left(\overrightarrow{c_{ik}}\right)^T \Delta\,[E_{DXi}] \\ -d_{il}\begin{bmatrix} S_{k1} & \cdots & S_{kn} \end{bmatrix} \\ [\Delta E_{SLi}]\,[b_i] \\ +d_{il}\left(\overrightarrow{c_{ik}}\right)^T [\Delta E_{RTi}]\,[b_i] \end{array}\right|_{x_m = x_m^{ideal}} \\ \text{and in which} \\ [a_i] = \left\{[I]_{n\times n} - [E_{SLi}]\,[S]\right\}^{-1}[I_i], \\ [b_i] = [S]\left\{[I]_{n\times n} - [E_{SLi}]\,[S]\right\}^{-1}[I_i] \\ [A] = \begin{bmatrix} [a_1] & \cdots & [a_n] \end{bmatrix}, \quad d_{ij} \in [D] = [A]^{-1} \end{cases} \tag{8}$$

while $\Delta S_{kl}\left(\Delta E_i\right)$ represents the deviation of S_{kl} caused by every error terms. $\overrightarrow{c_{ik}^T}$ represents the k^{th} row vector of matrix $[C_i] = \{[S]\,[E_{SLi}] - [I]\}\,[E_{RTi}]^{-1}$.

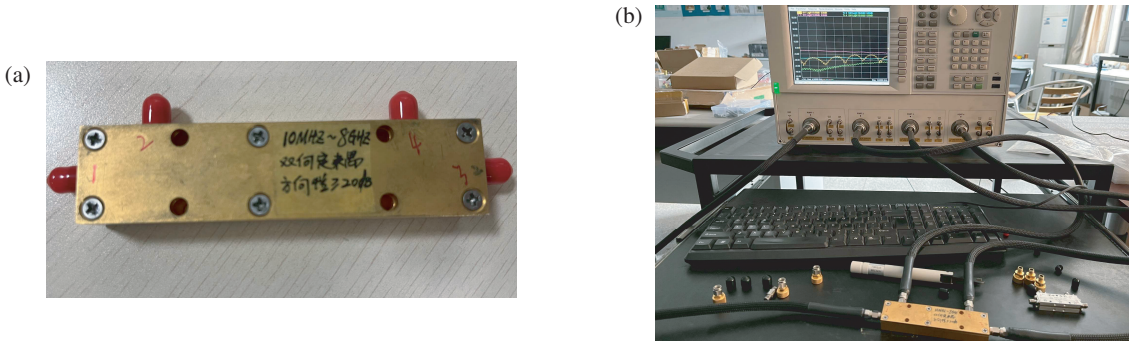

FIGURE 3. Measurement photograph. (a) DUT. (b) Agilent N5230C.

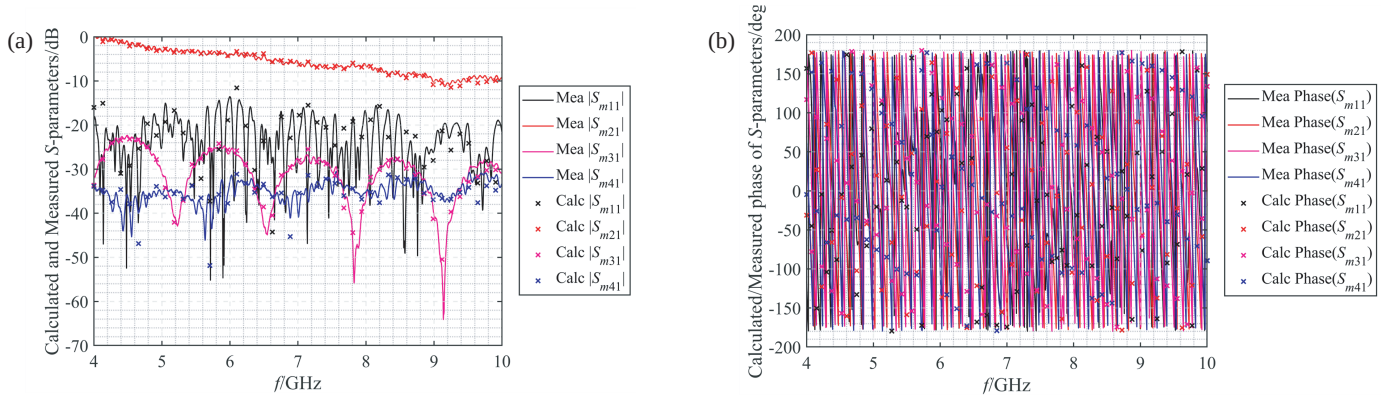

FIGURE 4. Calculated (Calc $S_{mii/ji}$) and measured (Mea $S_{mii/ji}$) raw S-parameters. (a) Magnitude. (b) Phase.

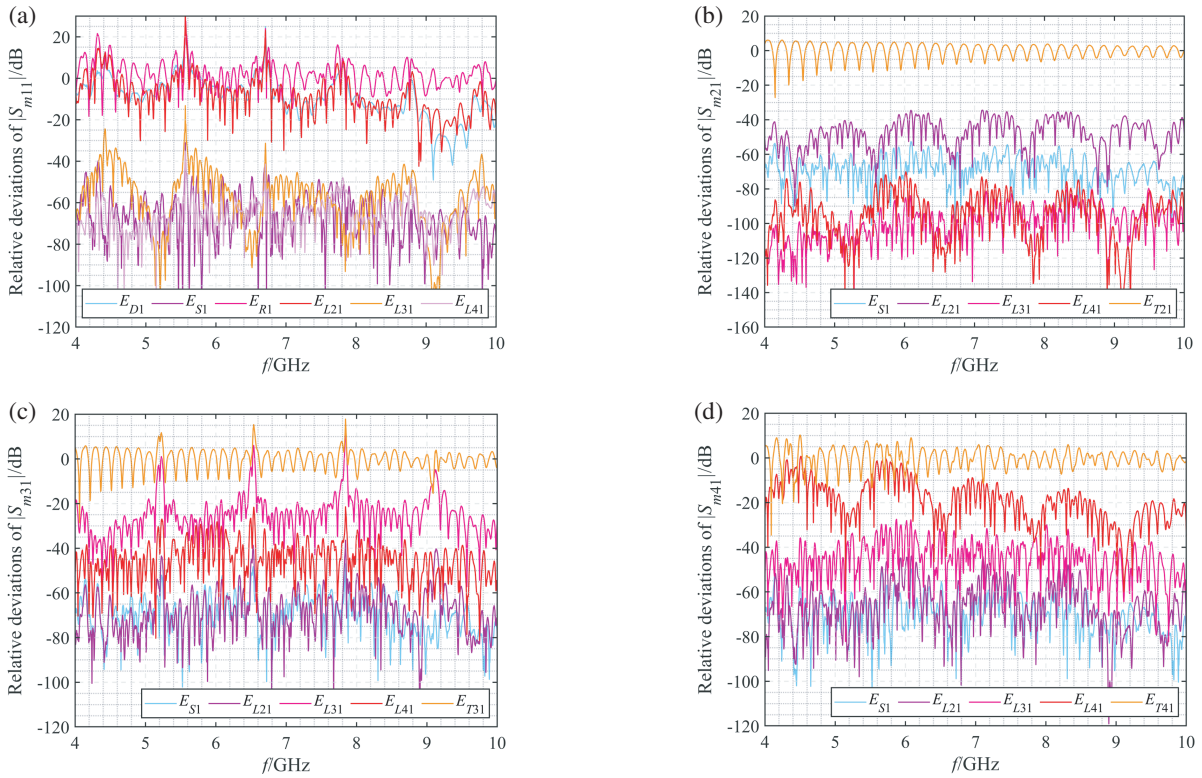

FIGURE 5. Deviations of raw measurement S-parameters. (a) Port 1 excitation. (b) Port 2 excitation. (c) Port 3 excitation. (d) Port 4 excitation.

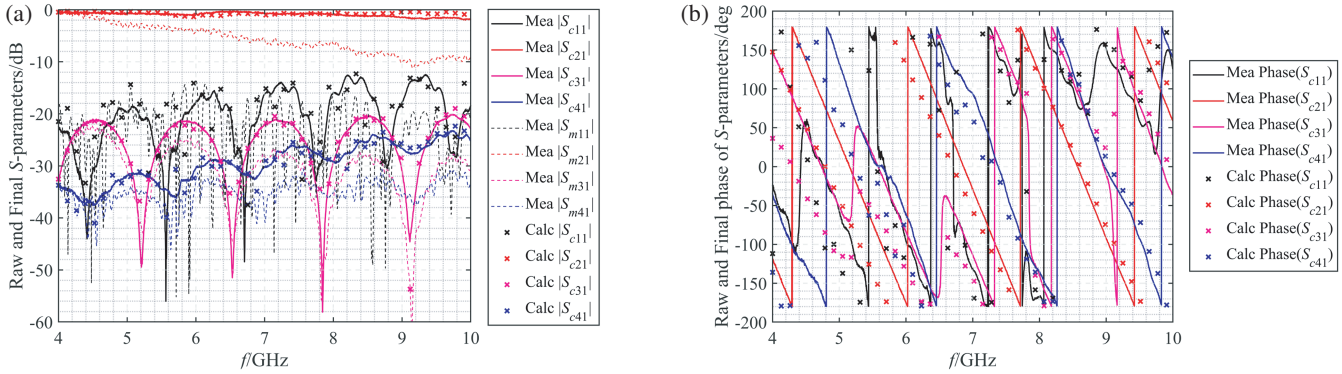

FIGURE 6. Calculated (Calc $S_{cii/ji}$) and measured (Mea $S_{cii/ji}$) final S-parameters. (a) Magnitude. (b) Phase.

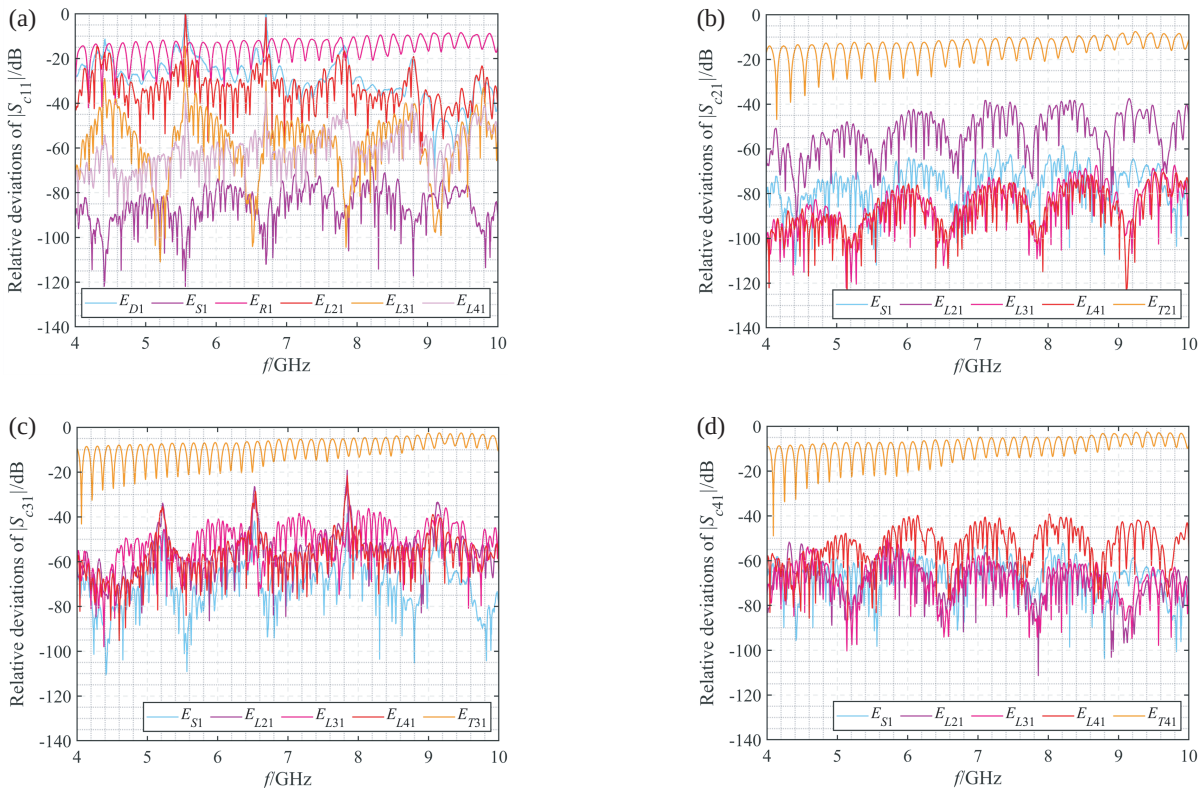

FIGURE 7. Deviations of final measured values of the 20 dB directional coupler. (a) Port 1 excitation. (b) Port 2 excitation. (c) Port 3 excitation. (d) Port 4 excitation.

3. EXPERIMENTAL MEASUREMENT

An MVNA (Agilent N5230C, as shown in Fig. 3(a)) is utilized to measure the DUT (a 20 dB direction coupler with known specifications, as shown in Fig. 3(b)). The MVNA is GSOLT-calibrated with calibration kit Ceyear AV20206. First, to verify the correctness of Equation (1), the calculated (Calc $S_{mii/ji}$) and measured (Mea $S_{mii/ji}$) raw S-parameters are plotted in Fig. 4. It is obvious that the calculated and measured results match well, which confirmed the correctness of Equation (1). The raw measurement deviations associated with error terms with different ports excited are extracted applying Equation (4) and shown in Fig. 5.

For the case of return loss S_{m11}, single port-related relative deviations are much more significant than other terms, about -20 to 20 dB. For transmission loss $S_{m21/31/41}$, the multiport-related relative transmission tracking errors are dominant factors that contribute to deviations, fluctuating from -20 to 0 dB while the load match errors are the second factors.

And, naturally, Equation (6) ought to be verified for effectiveness first, as a perquisite for the following analysis. The calculated (Calc $S_{cii/ji}$) and measured (Mea $S_{cii/ji}$) final S-parameters are plotted in Fig. 6. The deviations of final S-parameters are calculated after the MVNA is calibrated, as displayed in Fig. 7. After the GSOLT calibration, most deviations

TABLE 1. Comparison for raw and final deviation.

		MVNA	
Raw deviation	S parameter	Main contributor	Secondary contributor
	$\underline{S_{mii}}$	E_{Ri}	E_{Lji}
	$\underline{S_{mji}}$	E_{Tji}	E_{Lji}
Final deviation	S parameter	Main contributor	E_{Lji}
	$\underline{S_{cii}}$	E_{Ri}	E_{Lji}
	$\underline{S_{cji}}$	E_{Tji}	E_{Lji}

caused by error terms are degraded. The relative deviations of return loss S_{c11} caused by $E_{Di}/E_{Si}/E_{Ri}$ are reduced by 20 dB, which previously are main deviation contributors in raw results. The situation for transmission errors is similar, with the relative deviations caused by transmission tracking error decreasing by more than 20 dB. Overall, the GSOLT calibration turns out adequately efficient.

4. CONCLUSION

In this paper, a hardware-feature based deviation analysis is run by deriving the deviation related to every VNA hardware specification nonideality. During return loss measurement, single port-related deviations such as E_{Di}/E_{Ri} are the dominant factors, while for the case of transmission loss measurement, multiport deviations such as E_{Tji}/E_{Lji} are the main contributors. Among all these factors, E_R and E_T are frequency-independent error sources. Hence, a demand priority of actual MVNA specifications is presented, as a cost-effective guidance to design MVNA. A table for comprehensive comparison is given in Table 1.

REFERENCES

[1] Hackborn, R., "An automatic network analyzer system," *Microw. Journal*, Vol. 11, 45–52, May 1968.

[2] Stumper, U., "Influence of tmso calibration standards uncertainties on VNA S-parameter measurements," *IEEE Transactions on Instrumentation and Measurement*, Vol. 52, No. 2, 311–315, 2003.

[3] Stumper, U., "Uncertainty of VNA S-parameter measurement due to non-ideal TMSO or LMSO calibration standards," *Advances in Radio Science*, Vol. 1, 1–8, 2003.

[4] Stumper, U., "Influence of nonideal calibration items on S-parameter uncertainties applying the SOLR calibration method," *IEEE Transactions on Instrumentation and Measurement*, Vol. 58, No. 4, 1158–1163, 2008.

[5] Wang, M., Y. Zhao, T. H. Loh, Q. Xu, and Y. Zhou, "Efficient uncertainty evaluation of vector network analyser measurements using two-tier bayesian analysis and monte carlo method," *Proc. IET Conf.*, 1–5, 2018.

[6] Stumper, U., "Uncertainties of VNA S-parameter measurements applying the short-open-load-reciprocal (SOLR) calibration method," in *2008 Conference on Precision Electromagnetic Measurements Digest*, 438–439, 2008.

[7] Leinhos, J. and U. Arz, "Monte-Carlo analysis of measurement uncertainties for on-wafer thru-reflect-line calibrations," in *2008 71st ARFTG Microwave Measurement Conference*, 1–4, 2008.

[8] Zhao, W., X. Yang, J. Xiao, Q. H. Abbasi, H. Qin, and H. Ren, "Uncertainties of multiport VNA S-parameter measurements applying the GSOLT calibration method," *IEEE Transactions on Instrumentation and Measurement*, Vol. 61, No. 12, 3251–3258, 2012.

[9] Kruppa, W. and K. F. Sodomsky, "An explicit solution for the scattering parameters of a linear two-port measured with an imperfect test set," *IEEE Transactions on Microwave Theory and Techniques*, Vol. 19, No. 1, 122–123, 1971.

[10] Lenk, F., R. Doerner, and A. Rumiantsev, "Sensitivity analysis of S-parameter measurements due to calibration standards uncertainty," *IEEE Transactions on Microwave Theory and Techniques*, Vol. 61, No. 10, 3800–3807, 2013.

[11] Stumper, U., "Uncertainties of VNA S-parameter measurements applying the tan self-calibration method," *IEEE Transactions on Instrumentation and Measurement*, Vol. 56, No. 2, 597–600, 2007.

[12] Ouameur, M., F. Z. Bihan, and Y. Le, "Novel broadband calibration method of current shunts based on VNA," *IEEE Trans. Instrum. and Meas.*, Vol. 68, No. 3, 854–863, March 2019.

[13] Mubarak, F. A., R. Romano, G. Rietveld, and M. Spirito, "A novel calibration method for active interferometer-based VNAs," *IEEE Microwave and Wireless Components Letters*, Vol. 30, No. 8, 829–832, 2020.

[14] Stumper, U. and T. Schrader, "Influence of different configurations of nonideal calibration standards on vector network analyzer performance," *IEEE Transactions on Instrumentation and Measurement*, Vol. 61, No. 7, 2034–2041, 2012.

[15] Sanpietro, F., A. Ferrero, U. Pisani, and L. Brunetti, "Accuracy of a multiport network analyzer," in *Conference on Precision Electromagnetic Measurements*, Vol. 44, No. 2, 304–307, April 1995.

[16] Heuermann, H., "GSOLT: The calibration procedure for all multi-port vector network analyzers," in *IEEE MTT-S International Microwave Symposium Digest*, 1815–1818, Philadelphia, PA, USA, 2003.

[17] Ferrero, A., M. Garelli, B. Grossman, S. Choon, and V. Teppati, "Uncertainty in multiport S-parameters measurements," in *77th ARFTG Microwave Measurement Conference*, 1–4, 2011.